

Chemical Composition Influence on Macadam Surface Texture

Peng Tian^{a,b}, Lei Nie^{*a}, Gaofeng Zhan^{a,b}

^aCollege of Construction Engineering, Jilin University, Changchun 130026, China

^bJilin Jianzhu University, Changchun 130118, China

nielei@jlu.edu.cn

The difference of the macadam composition directly affects the texture characteristics of the macadam surface. Through the microscopic digital image analysis of macadam, this paper compares and analyses the distribution area ratio, perimeter, dendritic features and fractal features of main chemical components. Taking gravels of basalt, andesite and limestone as specimens, the author established a distribution model of texture features, and created 2D and 3D spaces based on the typical indices. The results show that: the basalt had limited dendritic structure, simple fractal, and smooth texture; the andesite had a wavy distribution of main components and an obvious dendritic structure; the limestone had a non-uniform distribution of main components, a large fractal value, and complex and changeable edges of principal components. This research proves that the 3D distribution space is an effective way to distinguish the texture features of the three types of rock, and lays a basis for the creation of 3D distribution model for the macadam texture characteristics.

1. Introduction

Macadam is a common material used in road construction. In asphalt mixtures, coarse aggregate mainly consists of gravel, macadam and slag with particle size greater than 2.36mm; in cement concrete, coarse aggregate mostly covers gravel and macadam with particle size greater than 4.75mm.

One of the most popular ways to investigate the macadam is the digital image analysis. This approach focuses on the distribution of coarse aggregates in the mixture (Chen et al., 2009), surface roughness (Anochie-Boateng et al., 2013), contour features (Shashidhar and Shenoy, 2002) and so on. Sometimes, the research focus is shifted to the composition and texture features of coarse aggregate (Masad, 2003).

Through the microscopic digital image analysis of macadam, this paper compares and analyses the distribution area ratio (Xie and Wang, 1999), perimeter, dendritic features (Koh et al., 2002) (Harvey et al., 2008) and fractal features of main components.

2. Preparations

2.1 Specimens

The gravels of basalt, andesite and limestone were taken as the specimens for our experiment. The macadam is obtained by crushing the rock with a crushed stone machine. In order to avoid the destruction of the original state, there is no treatment of the surface. Therefore, the flat original plane of macadam was chosen as the observation sample.

2.2 Composition of macadam

The basalt is an extrusive magmatic rock with a SiO₂ content of 45~52%. The main minerals are stone and plagioclase, plus a few quartz, alkali-feldspar and olivine. The andesite is an intrusive magmatic rock with a SiO₂ content of 53.5~62%. The main minerals are neutral-plagioclase and hornblende, plus some biotite. The limestone is carbonate rock with calcite as the main component, sometimes contains dolomite, clay minerals and clastic minerals. The main components of crushed stone is shown in Table 1.

Table 1: Original Images and Processed Images

No	crystalline mineral	phenocryst	calcite	agglutinate material
Basalt-01	50-70%	4-8%	-	-
Basalt-02	60%-80%	5-9%	-	-
Basalt-03	70-80%	3-7%	-	-
Andesite-01	-	15%-20%	-	-
Andesite-02	-	5%-8%	-	-
Andesite-03	-	8-10%	-	-
Limestone-01	-	-	0.9	0.05
Limestone-02	-	-	0.8	0.05
Limestone-03	-	-	0.87	0.07

3. Digital Image Acquisition

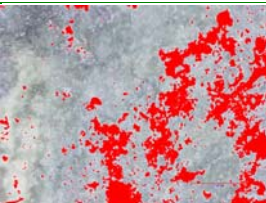
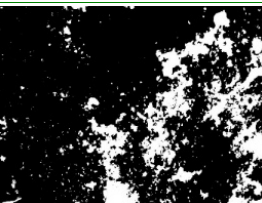
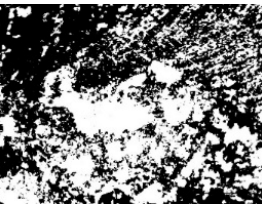
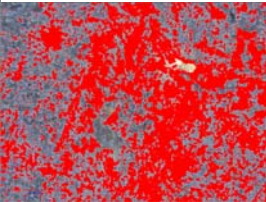
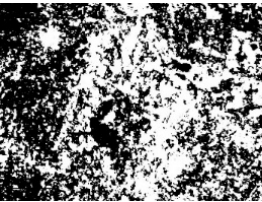
3.1 Equipment and settings

In our experiment, an HDMI digital microscope was adopted to capture digital images. The microscope is easy-to-use cutting edge device. The image sensor has a resolution of 5 million pixels, the manual focus range falls in 10mm~500mm, the maximum frame rate is 30f/s under 600 lush brightness, the magnification is 20~300 times. The capture images are stored in the format of JPEG. There are 8 LED light sources with controllable brightness.

3.2 Imaging

Three pieces of gravels were taken from each of the three types of stone to serve as experimental specimens. The observation surface was kept horizontal to avoid fuzziness during focusing (Baril et al., 2016). After a specimen was placed well, the calibration scale was placed on the flat surface to determine the observation rate and the target size (Han et al., 2016). In the experiment, the image was magnified 130 times. The original images are shown in column 1 of Table 2. The feature region selection and gradation is shown in column 2 and 3.

Table 2: Original Images and Processed Images

No	Captured images	Feature region selection	Gradation
Basalt			
Andesite			
Limestone			

As shown in the images, the basalt, an extrusive rock, carried expulsion features in its texture; the andesite, an intrusive rock, had fluid and wavy textures; the limestone, a cemented rock, was featured by a uniform texture distribution. The surface textures of the three kinds of rocks are so distinctive that they can be easily distinguished.

4. Texture Features

4.1 Area ratio and perimeter

The area distribution became clearer after the grey level processing (column 3, Table 1). The area ratio and perimeter are recorded in Table 3.

Table 3: Area and perimeter

No.	Area (Sum)	Per Area (Obj./Sum)	Perimeter (Sum)
Basalt-01	122943	0.1003	17502
Basalt-02	104905	0.0851	12146
Basalt-03	82543	0.0672	16224
Andesite-01	124250	0.1007	30365
Andesite-02	60679	0.0492	16016
Andesite-03	88905	0.0723	23986
Limestone-01	136139	0.1109	30276
Limestone-02	211044	0.1715	40944
Limestone-03	224378	0.1824	42291

However, it is difficult to ascertain the texture features of macadam solely based on the area and perimeter. Therefore, the author drew the scatter distribution with the area as the x-axis and the sum of perimeter as the y-axis. The three types of rock were differentiable to a certain extent, but not very clear as shown in Figure 1.

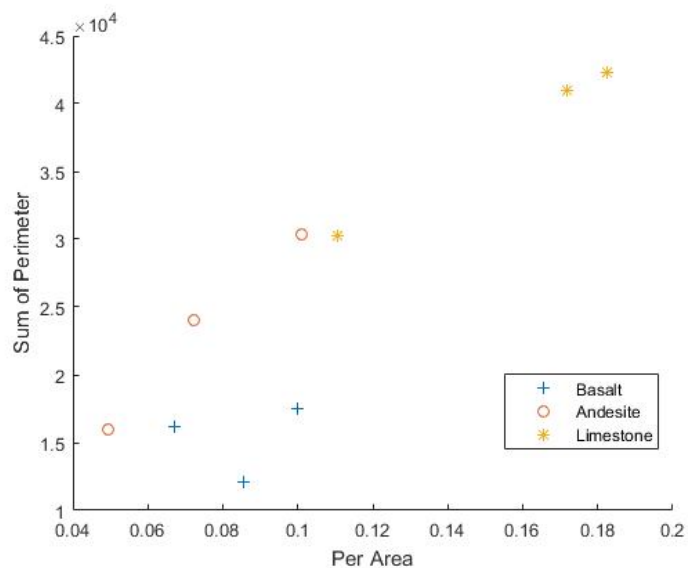


Figure 1: Scatter distribution of area and perimeter

4.2 Fractal geometry

Fractal geometry is a new branch of mathematics developed by the Benoit B. Mandelbrot (Sala, 2011) over two decades ago. Unlike traditional geometry, the fractal geometry is inspired by the chaotic, irregular and random natural phenomenon (Yu and Xie, 2016). Despite the lack of strictly mathematical fractal in nature, it is possible to build an approximate fractal model for some objects with fractal features. In this way, these objects can be analysed from the perspective of fractal.

The dimension, essential to the fractal geometry, describes how much space is occupied by a collection (Li et al., 2016). The concept is defined in various ways (Li and Li, 2016), such as Hausdorff dimension, box-counting dimension, modified box-counting dimension, packing dimension and so on (Luo and Ren, 2016). Among them, the mathematical calculation and empirical estimation of box-counting dimension is relatively easy to use. Therefore, the fractal dimension is generally referred to as the box-counting dimension. The fractal geometry dimensions of macadam surface is shown in Table 4.

Table 4: Box-counting dimension and dendritic

No.	fractal dimensions (Mean)	Dendrites (Sum)
Basalt-01	1.149045511	78
Basalt-02	1.158506460	63
Basalt-03	1.140964013	66
Andesite-01	1.184570108	242
Andesite-02	1.158969874	94
Andesite-03	1.175797172	177
Limestone-01	1.164983894	132
Limestone-02	1.173917737	176
Limestone-03	1.173603413	236

4.3 Dendritic features

In the field of medicine, the branch of cell body extension is called dendritic (Zhang, 2016). According to the microscopic images (Figure 2), the texture of the rough aggregate surface (Choudhury, 2016) also carries the dendritic features.

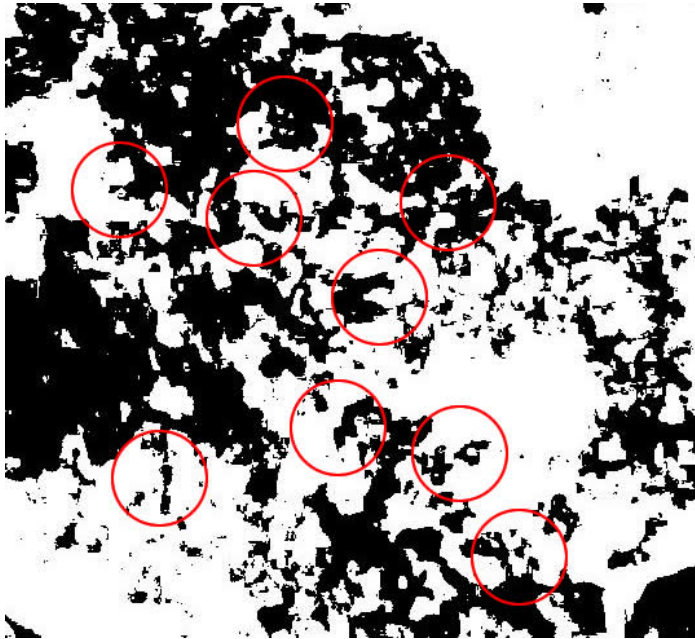


Figure 2: Dendrites in texture

Although the dendrites could not transmit the information as cells, the approximate shape reflects the feature variation of the stone texture. Each dendritic texture forms a whole, stretching out irregularly. By recognizing dendritic textures, the number of dendrites in the macadam surface is listed in Table 4.

Because the eigenvalues are all from the texture of the macadam surface, there is an inevitable connection between them (Trawiński et al., 2016) (Beloborodov et al., 2016). Therefore, the author drew the scatter distribution with the sum of dendrites as the x-axis and the mean of fractal dimension as the y-axis. It can be seen that the scatter distribution of andesite and limestone was approximately linear as shown in Figure 3.

The sum of dendrites was proportional to the mean of fractal dimension. By contrast, the distribution of basalt did not obey the linear distribution. The difference is attributable to the genesis of the rock. Since basalt is formed in a much longer time than the other two stones, it has a more complex texture, as evidenced by the greater sum of dendrites and mean of fractal dimension.

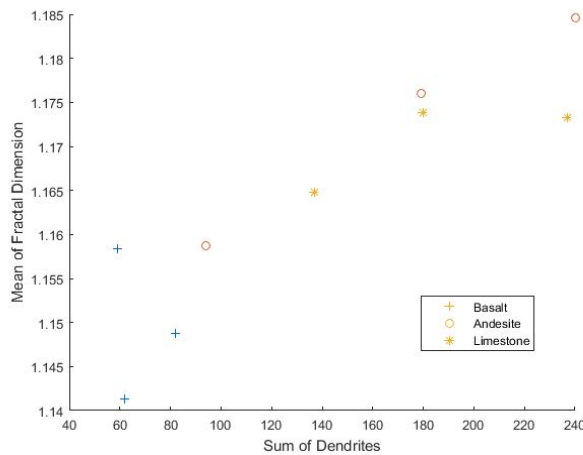
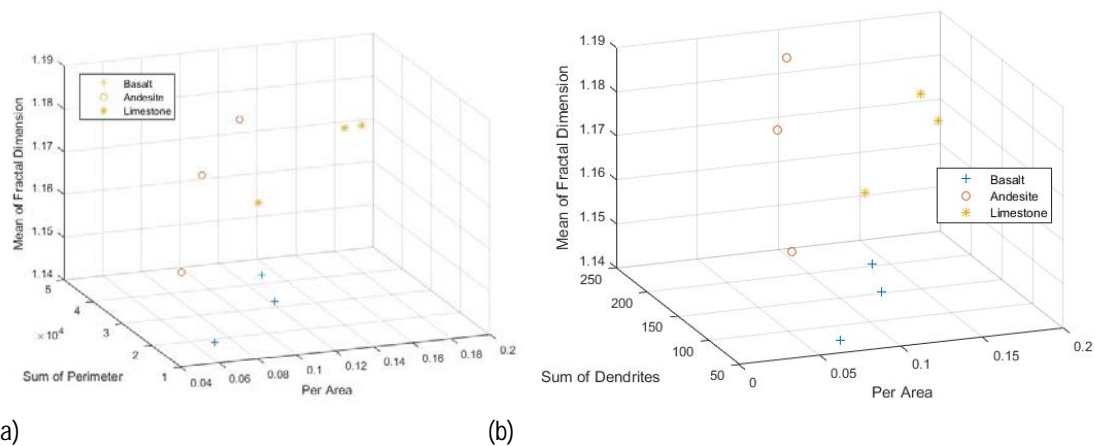


Figure 3: Scatter distribution of fractal dimension and sum of dendrites

4.4 3D distribution model

The 2D distribution map based on two indices is not sufficient for the differentiation of texture features among the three types of macadam. Therefore, a 3D distribution model was created (Figures 4) with three indices acting as the axes x, y and z.



(a)

(b)

Figure 4: 3D scatter distribution of characteristic parameters

In the 3D scatter distribution, the three types of macadam had no overlap on the distribution of texture features. The basalt was relatively small in terms of fractal value, the sum of dendrites and mean of fractal dimension. The andesite shared a similar area with the basalt, but differed greatly in the fractal value; the limestone boasted a relatively high value for almost every index. That is inseparable from the chemical composition of the macadam.

The basalt is an extrusive rock. The composition of crystalline minerals accounts for 70% to 90%. The andesite is an intrusive rock, had fluid and wavy textures. The proportion of phenocryst is higher. The limestone is a cemented rock, was featured by a uniform texture distribution. The calcite is the main composition, has a lot of pores.

5. Conclusion

The distinct texture features of macadam are closely related to the main chemical composition and formation process. The distribution of the main components can be clearly distinguished on the digital image. The characteristic parameters of the distribution region reflect the content, distribution, proximity-relation and forming process of the main components for each type of the macadam

The basalt, an extrusive rock, had small index values: the dendritic structure was limited, the fractal was simple and the texture was smooth; the andesite, an intrusive rock with a slow forming process, had a wavy distribution of main components and an obvious dendritic structure; the limestone, a cemented rock, carried a non-uniform distribution of main components, a large fractal value, and complex and changeable edges of principal components.

Moreover, the 3D distribution space was proved as an effective way to distinguish the macadam texture features. This research lays a solid basis for the creation of 3D distribution model for the texture features of coarse aggregate. Based on this model, it is possible to study the adhesion of asphalt to the surface of macadam and provide support for the performance analysis of the macadam mixture.

Acknowledgments

This study was supported by the 13th Five-Year science of the Education Department in Jilin Province, Jilin Education Science Planning Project (GH150340) and technology research project planning 2017 in Jilin provincial industrial innovation special fund project (2017C030-3).

Reference

- Anochie-Boateng J.K., Komba J.J., Mvelase G.M., 2013, Three-dimensional laser scanning technique to quantify aggregate and ballast shape properties, *Construction and Building Materials*, 43, 389-398.
- Baril M.A., Sorelli L., Réthoré J., Baby F., Toutlemonde F., Ferrara L., Bernardi S., Fafard M., 2016, Effect of casting flow defects on the crack propagation in UHPFRC thin slabs by means of stereovision Digital Image Correlation, *Construction and Building Materials*, 129, 182-192.
- Beloborodov R., Pervukhina M., Luzin V., Delle P. C., Clennell M. B., Zandi S., Lebedev M., 2016, Compaction of quartz-kaolinite mixtures: The influence of the pore fluid composition on the development of their microstructure and elastic anisotropy, *Marine and Petroleum Geology*, 78, 426-438.
- Chen G.M., Zhou C.X., Tan Y.Q., 2009, Fractal evaluation of surface texture for coarse aggregate and performance test of asphalt mixture, *Journal of Traffic and Transportation Engineering*, 9, 1-5.
- Choudhury A., Medioni G., 2013, Hierarchy of non-local means for preferred automatic sharpness enhancement and tone mapping, *Journal of the Optical Society of America A Optics Image Science & Vision*, 30, 353-366
- Han J., Wang K., Wang X., Monteiro P.J.M., 2016, 2D image analysis method for evaluating coarse aggregate characteristic and distribution in concrete, *Construction and Building Materials*, 127, 30-42.
- Harvey C. D., Yasuda R., Zhong H., Svoboda K., 2008, The Spread of Ras Activity Triggered by Activation of a Single Dendritic Spine, *Science*, 321, 136-140.
- Koh I.Y., Lindquist W. B., Zito K., Nimchinsky E. A., Svoboda K., 2002, An image analysis algorithm for dendritic spines, *Neural Computation*, 14, 1283-1310.
- Li W., Li Q., 2016, Reform on mathematical modelling teaching contents in the era of big data, *Advances in Modelling and Analysis A*, 53, 129-144.
- Li Z.X., Li C., Jue Z., 2016, Multi-objective particle swarm optimization algorithm for recommender system, *Advances in Modelling and Analysis B*, 59, 189-200.
- Luo L.J., Ren H.P., 2016, A new similarity measure-based MADM method under dynamic interval-valued intuitionistic fuzzy environment, *Advances in Modelling and Analysis A*, 53, 84-92.
- Masad E., 2003, The development of a computer controlled image analysis system for measuring aggregate shape properties, *Transportation Research Board*. Washington. DC, United States, 5-7.
- Sala, N., 2011, Fractal geometry in computer graphics and in virtual reality, *Computer Graphics*, 163-177.
- Shashidhar N., Shenoy A., 2002, On Using Micromechanical Models to Describe Dynamic Mechanical Behavior of Asphalt Mastics, *Mechanics of Materials*, 34, 657-669.
- Trawiński W., Bobiński J., Tejchman J., 2016, Two-dimensional simulations of concrete fracture at aggregate level with cohesive elements based on X-ray μ CT images, *Engineering Fracture Mechanics*, 168, 204-226.
- Xie H., Wang J. A. 1999. Direct Fractal Measurement of Fracture Surfaces, *International Journal of Solids & Structures*, 36, 3073-3084.
- Yu W.B., Xie J.Y., 2016, Bayesian estimation of reliability of geometric distribution under different loss functions, *Advances in Modelling and Analysis A*, 53, 172-185.
- Zhang K., Huang D., Zhang B., Zhang D. S., 2016. Improving texture analysis performance in biometrics by adjusting image sharpness, *Pattern Recognition*, 66, 16-25.